Degradation of azo dye active brilliant red X-3B by composite ferrate solution

G.R. Xu [*], Y.P. Zhang, G.B. Li

State Key Laboratory of Urban Water Resource and Environment, Harbin Institute of Technology,P.O. Box 2602, 202 Haihe Road, Nangang District, Harbin, Heilongjiang Province, Postal code 150090, China

ARTICLE INFO

ABSTRACT

Composite ferrate(VI) solution (CFS) with improved stability was successfully prepared in this study. The stability of Fe(VI) increased from hours for potassium ferrate at pH 9–10 to 16 d for 1 mmol L^{-1} Fe(VI) in CFS at 25 °C, decomposing 24%. The Fe(VI) was more stable at low concentration (1 mmol L^{-1}) than that at high concentration (10 mmol L^{-1}). The degradation of the azo dye reactive brilliant red X-3B (X-3B) by CFS was investigated. The results showed that pH, initial dye concentration and CFS dosage affected the degradation efficiency. For 0.08 mmol L^{-1} X-3B simulate wastewater, the optimal pH and CFS dosage were 8.4 and 25 mg L^{-1} (as K$_2$FeO$_4$), and about 99% X-3B was decolorized after 20 min under this conditions. The color decay was considerably faster than the decrease in COD and TOC, which was attributed to the ease of chromophore destruction. Compared with the decolorization, the removal percentage of COD and TOC were 42% and 9% after 60 min, respectively. The Fe(VI) and ClO$^-$ were contained in CFS, which have synergetic effect for the degradation of X-3B. Additionally, phthalic acid and muconic acid were identified as intermediates by GC/MS, which was in accordance with the lowered pH with the reaction time. The complete mineralization of X-3B cannot be achieved under the oxidation by CFS. And a tentative pathway for the oxidative degradation of X-3B was postulated.

1. Introduction

Synthetic dyes have been widely used in textile, paper, photographic and coating industries etc. [1]. In textile industry, it was estimated that about 10–15% of dyes were lost during the dying process and released as effluents [2]. These compounds are highly colored and can heavily contaminate water source. With azo group bound to aromatic rings, azo dyes are an important class of synthetic dyes which constitute threat to environment owing to their non-biodegradability, toxicity and potential carcinogenic nature [3]. Therefore, chemical degradation of azo dyes has attracted much attention in recent years. Different oxidation technologies have been studied for the degradation of azo dyes in wastewater, such as H$_2$O$_2$-based oxidation [4,5], catalytic ozonation [6], photocatalysis [7,8], ultrasonic irradiation [9], and electrochemical oxidation [10]. However, as far as is known, little has been reported on the degradation of azo dyes in general by potassium ferrate.

Potassium ferrate has been found to be a powerful oxidant over a wide pH range and many studies have considered its role as an oxidant in water and wastewater treatment [11]. During the aqueous oxidation reaction, Fe(VI) is reduced to a non-toxic by

product, Fe(III), which makes Fe(VI) an environmentally friendly oxidant for water treatment processes [12,13]. The redox potential of ferrate ranges from +2.20 V to +0.72 V in acidic and basic solutions, thus its redox potential in acidic solution is the strongest of all the oxidants used in water and wastewater treatment, including ozone and hydrogen peroxide. Many organic contaminants as phenols and phenolic endocrine-disrupting chemicals [14,15], thioacetamide [16], sulfur-containing [17] and nitrogen-containing pollutants [18] can be effectively degraded by ferrate in water and wastewater treatment. In this paper, composite ferrate solution (CFS) with improved stability was prepared by modified chemical method with KOH at 65 °C. For eliminating the precipitation and purification processes needed for solid potassium ferrate synthesis, the preparation process for CFS is simple, time saving and low cost. On this basis, the CFS oxidation technology for degradation of azo dyes in wastewater was proposed. Active brilliant red X-3B (X-3B), one of the familiar azo dyes, was chosen as a probe molecule in this work.

2. Materials and methods

2.1. Materials and reagents

Composite ferrate solution was prepared by the modified chemical oxidation method: Fe(NO$_3$)$_3$·9H$_2$O reacted with ClO$^-$ in

* Corresponding author. Tel.: +86 45186282559; fax: +86 45186282559.
E-mail addresses: xgr@hit.edu.cn, xgr099@yahoo.cn (G.R. Xu).

5.3 mol L^{-1} KOH media at 65 °C, after 60 min, CFS with higher Fe(VI) concentration and improved stability was obtained. The CFS was diluted, then filtered by funnel (G$_4$) and stored in polyethylene plastic bottle at 4 °C. Solid phase potassium ferrate was prepared and the purity of the product was determined by chromite method and found to be 93%.

The dye of reactive brilliant red X-3B was purchased from the eighth dye chemical factory of Tianjin, China, and used directly without further purification. All other chemicals were of reagent grade, and used as received.
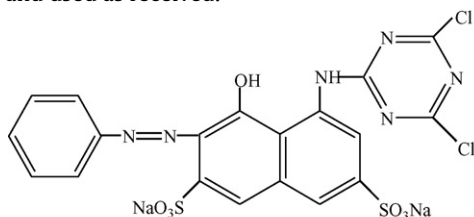
Reactive Brilliant Red X-3B
(chemical formula=C$_{19}$H$_{10}$O$_7$N$_6$Cl$_2$S$_2$Na$_2$, MW=615.34)

2.2. Decomposition of Fe(VI) in CFS

Taking 100 mL CFS samples with different initial Fe(VI) concentrations, as 1 mmol L^{-1}, 5 mmol L^{-1} and 10 mmol L^{-1}, into glass vessels, and stored at 25 °C in a water bath. The decomposition of Fe(VI) was monitored by determining the Fe(VI) concentration at intervals of 24 h. As a comparison, similar decomposition tests were carried out in which solid potassium ferrate was dissolved in distill water to produce ferrate concentration of 0.29 mmol L^{-1}, and the pH values (pH 9, 10) of ferrate solutions were controlled with borate–potassium chloride–sodium hydroxide buffer solution, which have been reported to be the stable pH ranges for ferrate ion [19].

2.3. Degradation of X-3B by CFS

In each experiment, 100 mL dye solution with the concentration of 0.08 mmol L^{-1} was used. The oxidation tests were carried out by rapid mixing of the two chemical solutions (X-3B and CFS), and then adjusted the pH value by H$_2$SO$_4$ quickly. In the oxidation tests, samples were taken periodically up to 60 min. At each sampling time, sodium sulfite solution was added immediately to the sample when it was taken to stop any further reaction (except for COD measurement). The samples were then filtered by 0.45 μm pore size nylon membrane filter before analysis. All the experiments were carried out at room temperature (23 ± 2 °C).

2.4. Analytical methods

In this study, the concentration of Fe(VI) in CFS was determined by monitoring the absorbance at 510 nm [20] using a 752 spectrophotometer (China), and calculated according to the calibration curve. X-3B concentration was determined by its absorbance at 540 nm [21] and calculated according to the calibration curves. The interference from Fe(VI) was removed as following: after adding sodium sulfite the residual Fe(VI) will be reduced to Fe(III), and some Fe(III) will be removed by 0.45 μm filter as Fe(OH)$_3$. The residual Fe(III) in the solution also has absorbance at 540 nm, which has been measured for the blank test and subtracted by the absorbance of X-3B. The pH values of solutions were recorded by pH analyzer (PHS-3C, China). The COD were determined at 620 nm after 2 h reaction in the COD reactor (HACH, America). The TOC was measured with TOC-V$_{CPN}$ total organic carbon analyzer (Shimazu,
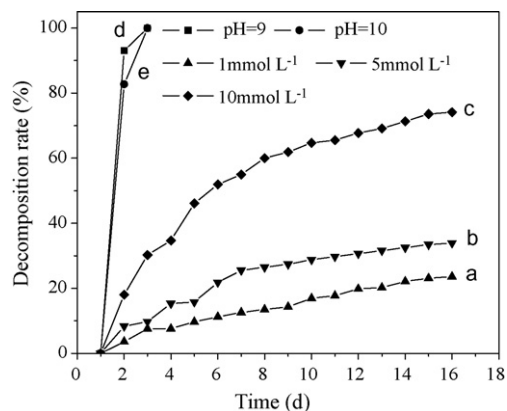

Fig. 1. Stability of Fe(VI) in CFS with different initial Fe(VI) concentrations at 25 °C: (a) pH 12.6 + CFS = 1 mmol L^{-1}; (b) pH 13.3 + CFS = 5 mmol L^{-1}; (c) pH 13.6 + CFS = 10 mmol L^{-1}; and compared with K$_2$FeO$_4$ solution at (d) pH 9 and (e) pH 10 with initial Fe(VI) concentration of 0.29 mmol L^{-1}.

Japan). The samples of reaction for 1 min, 5 min, 15 min, 30 min and 60 min were combined to detect the intermediates of X-3B by GC/MS (6890GC/5973MSD) (Agilent, America) after esterification and extraction. In this work, the mixed degradation products were esterified with methanol at 60 °C for 2 h in presence of concentrated sulfuric acid and extracted with MTBE. GC analysis was equipped with a DB-5 column (30 m × 0.25 mm × 0.25 μm) and interfaced directly to the MS. The GC column was operated for 4 min at a temperature of 50 °C, which was then increased to 250 °C at the rate of 10 °C min^{-1}, and then it was increased to 280 °C at the rate of 25 °C min^{-1}, the final temperature was 300 °C and kept for 5 min.

3. Results and discussion

3.1. Fe(VI) stability in CFS

It is well known that ferrate is unstable in aqueous solution, and will quickly reduce to Fe(III) or insoluble end-product, (Fe[OH]$_3$). But in this study, the stability of Fe(VI) in CFS have been greatly improved, as shown in Fig. 1. It was clear that the stability of Fe(VI) in CFS was more stable than that prepared with potassium ferrate solid at pH 9 and pH 10. The decomposition rate of 1 mmol L^{-1} Fe(VI) in the CFS was 4% after being stored for 1 d and 24% for 16 d at 25 °C. While for the 0.29 mmol L^{-1} potassium ferrate solution, about 93% (pH 9) and 83% (pH 10) were decomposed after 1 d. The Fe(VI) in CFS was highly initial ferrate concentration dependent, for the initial Fe(VI) concentrations of 1 mmol L^{-1}, 5 mmol L^{-1} and 10 mmol L^{-1} the decomposition rates after 16 d were 24%, 34% and 74%, respectively.

The ferrate has a high redox potential that leads to rapid redox reactions with water to produce oxygen and Fe(III) (Eq. (1)). It makes the ferrate solution unstable.

$$4K_2FeO_4 + 10H_2O \rightarrow 4Fe(OH)_3 + 8KOH + 3O_2\uparrow \qquad (1)$$
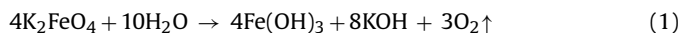
While in CFS, hypochlorite existed which has higher redox potential (0.841 V) in strong alkaline solution and can oxidize Fe(III) to Fe(VI) (Eq. (2)). Consequently, it retarded the ferrate decomposition rate and enhanced its stability. On the other hand, under the effect of light and heat, ClO$^-$ can decompose into Cl$^-$ and active oxygen ([O]) (Eq. (3)), the active oxygen also has higher oxidation potential. It is found that active oxygen also is produced during the degradation of Fe(VI), seen as Eqs. (4)–(8) [22]. Therefore, the [O] produced from ClO$^-$ in CFS inhibits the reaction of Eq. (5), and consequently it promotes the stability of Fe(VI). If there were no
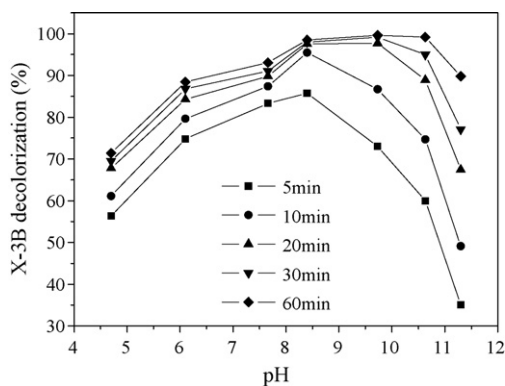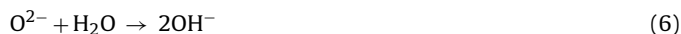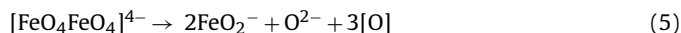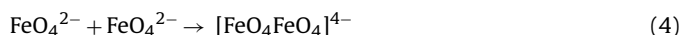
Fig. 2. Effect of pH on the decolorization of X-3B by CFS with dosage of 25 mg L^{-1} K$_2$FeO$_4$, and with initial X-3B concentration of 0.08 mmol L^{-1}.

Fig. 3. Effect of CFS dosage (as K$_2$FeO$_4$) on the decolorization of X-3B at pH 8.5 with initial X-3B concentration of 0.08 mmol L^{-1}.

ClO$^-$ in Fe(VI) solution, just as pure potassium ferrate solution, only the decomposition reaction of Fe(VI) (as Eq. (1)) occurred, and the Fe(VI) degraded quickly. So the Fe(VI) in CFS could persist much longer as indicated in Fig. 1.

$$2Fe(OH)_3 + 3ClO^- + 4OH^- \rightarrow 2FeO_4^{2-} + 3Cl^- + 5H_2O \qquad (2)$$

$$ClO^- = Cl^- + [O] \qquad (3)$$

$$FeO_4^{2-} + FeO_4^{2-} \rightarrow [FeO_4FeO_4]^{4-} \qquad (4)$$

$$[FeO_4FeO_4]^{4-} \rightarrow 2FeO_2^- + O^{2-} + 3[O] \qquad (5)$$

$$O^{2-} + H_2O \rightarrow 2OH^- \qquad (6)$$

$$FeO_2^- + H_2O \rightarrow Fe(O)(OH) + OH^- \qquad (7)$$

$$2[O] \rightarrow O_2 \qquad (8)$$

3.2. Effect of pH on the decolorization of X-3B by CFS

The pH had a great effect on the decolorization of X-3B by CFS, and the results were shown in Fig. 2. It was clear that the optimal pH range for the decolorization was pH 8.4–10.6. The decolorization efficiency of X-3B could reach 99% after 60 min, but the reaction rate at pH 8.4 was faster than that at pH 10.6. The decolorization of X-3B at this pH range maybe explained by the higher redox potential and more stability of Fe(VI). The decolorization efficiency of X-3B was gradually lower when pH overpassed 10.6 owing to the relatively low redox potential of ferrate and hypochlorite contained in CFS. When pH lowered to 8.4, the degradation of X-3B reduced. The minor decolorization efficiency of X-3B was obtained at pH 4.7, as 71%. Although the redox potential of ferrate and hypochlorite increase with pH decrease, the rate of ferrate decomposition is
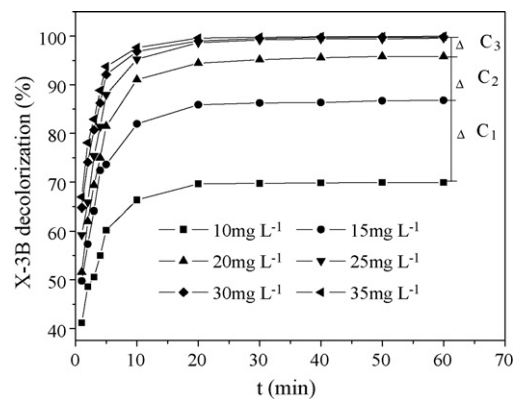
accelerated at the same time. It will cause part of Fe(VI) to reduce to Fe(III) before it reacts with X-3B, and leads the decolorization of X-3B to decrease. On the other hand, the triazine ring contained in X-3B structure has strong function of electron withdrawing, which causes the adjacent benzene ring to lack electron. It will lead the formula structure to be attracted by electron and take nucleophilic substitution reaction. While the almost total ClO$^-$ exists as HClO when pH lowers to 6, which reduces the chance of hypochlorous attacking the formula structure of the azo dye and reduces the degradation of X-3B.

It was possible that the maximal X-3B decolorization at pH 8.4 might also reflect the importance of X-3B adsorbance on to insoluble Fe(III) species, given that Fe(III) had a minimum solubility at pH 8.4. However, it was believed that this was not an important effect since Fe(III) solubility did not vary substantially within the 7–10 pH range.

3.3. Effect of CFS dosage on the decolorization of X-3B

The dosage of CFS was found to be the most important factor to achieve better degradation of X-3B. Different CFS dosages (as K$_2$FeO$_4$) were employed under same conditions, and the results were shown in Fig. 3. It was clear that the decolorization efficiency of X-3B increased with the CFS dosage, and the optimal CFS dosage was 25 mg L^{-1} K$_2$FeO$_4$. Under this condition, 99% X-3B was decolorized after 20 min. The decolorization efficiency of X-3B changed little with the reaction time after 20 min, and about 90% of X-3B was degraded at first 5 min. The initial rate increased slightly with the CFS dosage (Fig. 4a(i)), which could be explained that increase of CFS dosage would promote the collision frequency between oxi-
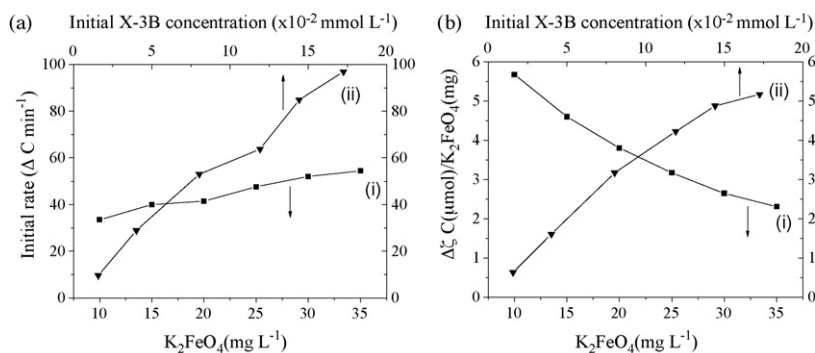

Fig. 4. The initial rate (a) and the oxidant load (b) as functions of CFS dosage and initial X-3B concentration at pH 8.5. The initial rate was expressed by the decreased X-3B concentration (ΔC) per minute; the oxidant load was expressed by the amount of X-3B degraded by unit CFS, calculated as K$_2$FeO$_4$.
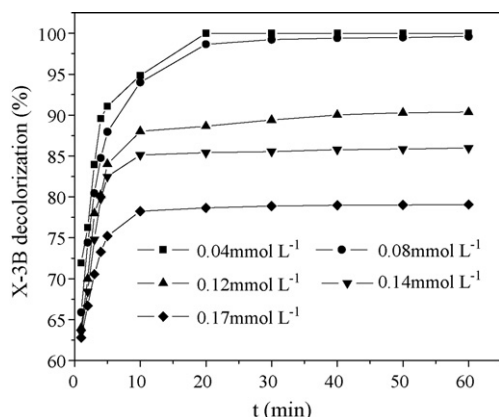
Fig. 5. Effect of dye initial concentration on the decolorization of X-3B by 25 mg L^{-1} CFS at pH 8.5.

dants and X-3B, and then increase the reaction rate. The amount of degraded X-3B ($\triangle C$) between the two near CFS dosages decreased with the CFS dosage (Fig. 3), and also did the oxidant load (the amount of X-3B degraded by unit CFS, calculated as K$_2$FeO$_4$) (Fig. 4b(i)). The unequal $\triangle C$ and decreased oxidant load were caused by (1) the rapid decomposition rate of Fe(VI) with the initial Fe(VI) concentration increase; (2) the reaction between Fe(VI) and the oxidation products of X-3B; and (3) the overdose of CFS. The maximum oxidant load (the maximum amount of X-3B degraded by unit CFS, calculated as K$_2$FeO$_4$) of 5.7 μmol X-3B/1 mg K$_2$FeO$_4$ was found at 10 mg L^{-1} K$_2$FeO$_4$ of CFS.

3.4. Effect of initial dye concentration on the decolorization of X-3B

Fig. 5 showed the effect of dye initial concentration on the decolorization of X-3B by CFS. The results displayed that the decolorization efficiency decreased from 100% to 79% when the initial X-3B concentration increased from 0.04 mmol L^{-1} to 0.17 mmol L^{-1}. But the initial rate (Fig. 4a(ii)) and oxidant load (Fig. 4b(ii)) increased with that. The effect of initial dye concentration on the initial rate was greater than that of CFS dosage. It indicated that increase of initial dye concentration not only could promote the collision frequency between the oxidants and X-3B, but also reduced the side reaction which was different from increasing oxidant concentration. The maximum oxidant load was 5.2 μmol X-3B/1 mg K$_2$FeO$_4$ found at 0.17 mmol L^{-1} X-3B initial concentration, which was close to 5.7 μmol X-3B/1 mg K$_2$FeO$_4$ gotten from above.

3.5. Synergetic effect of Fe(VI) and ClO$^-$

The Fe(VI) and ClO$^-$ are both strong oxidants and contained in CFS. The degradation of X-3B by K$_2$FeO$_4$ and NaClO were performed to compare with CFS, and the results were shown in Figs. 6 and 7. The dosage of K$_2$FeO$_4$ and NaClO were consistent with that contained in CFS, as 25 mg L^{-1} and 20 mg L^{-1}, respectively.

Fig. 6 clearly showed that CFS reaction system had the best decolorization efficiency, and K$_2$FeO$_4$ was better than NaClO. The decolorization efficiencies for CFS, K$_2$FeO$_4$ and NaClO were 91%, 74% and 47% (after 5 min), and 98%, 80% and 66% (after 20 min), respectively. K$_2$FeO$_4$ and NaClO did not have synergetic effect for decolorization. It may be due to that both K$_2$FeO$_4$ and NaClO could break azo bond quickly, and the competition reaction existed between them. It caused a portion of oxidant to react with oxidation products of X-3B or degrade by itself, which lowered the decolorization efficiency.
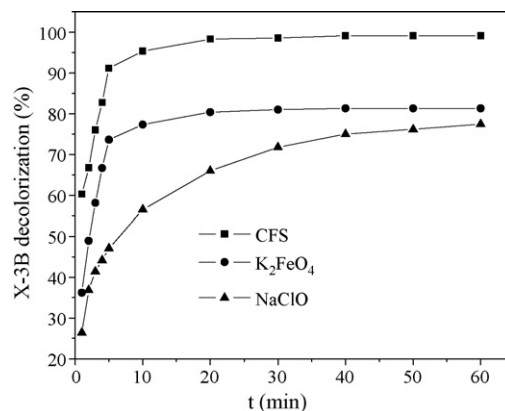

Fig. 6. The decolorization efficiencies of X-3B oxidized by CFS, K$_2$FeO$_4$ and NaClO. Conditions: pH 8.5; C_{X-3B} 0.08 mmol L^{-1}; CFS 25 mg L^{-1}; K$_2$FeO$_4$ 25 mg L^{-1}; NaClO 20 mg L^{-1}.

The COD removal percentage by CFS, K$_2$FeO$_4$ and NaClO were displayed in Fig. 7, and the initial COD was 25.4 mg L^{-1}. The results indicated that the COD removal percentage by K$_2$FeO$_4$ and NaClO were 20% and 16% (after 60 min), respectively. The low COD removal percentage by NaClO is in accordance with literature reported [23]. About 42% COD could be effectively removed by CFS, which was greater than that of K$_2$FeO$_4$ plus NaClO. Therefore, K$_2$FeO$_4$ and NaClO had synergetic effect for COD removal.

Except for the oxidants of Fe(VI) and NaClO in CFS, Fe(V) and Fe(IV) could be generated during the oxidation by decomposition of Fe(VI) [24,25]. Both Fe(V) and Fe(IV) have been reported as highly reactive oxidation states due to the partial free-radical character of Fe(V) (Fe^V=O $\leftrightarrow$ Fe^{IV}–O$^\bullet$), and they can also degrade X-3B.

3.6. pH change with reaction time

The pH values of solutions oxidized by CFS, K$_2$FeO$_4$ and NaClO were determined and the results were shown in Fig. 8. Fig. 8 indicated that for CFS reaction system the pH value increased slowly at the first 5 min from 9.00 to 9.16, then it decreased with the reaction time prolonged. The pH value decreased to 8.30 at 60 min. It is well known that higher OH$^-$ ions concentration will be produced during the oxidation and degradation of K$_2$FeO$_4$, which will lead the pH value to increase. The pH value increased quickly from 8.28 to 9.75 when the reaction time prolonged from 0 min to 15 min in K$_2$FeO$_4$ reaction system (Fig. 8), which approved it. On the other
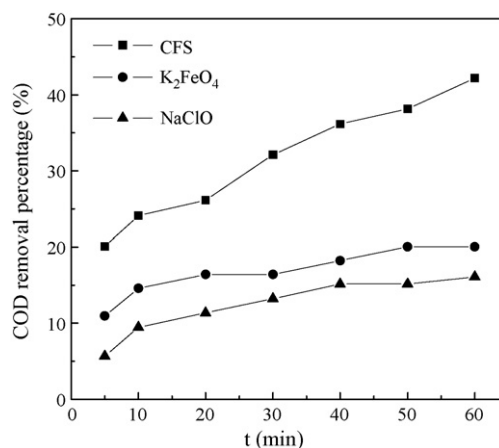

Fig. 7. The COD removal percentage of X-3B oxidized by CFS, K$_2$FeO$_4$ and NaClO. Conditions: pH 8.5; COD 25.4 mg L^{-1}; CFS 25 mg L^{-1}; K$_2$FeO$_4$ 25 mg L^{-1}; NaClO 20 mg L^{-1}.
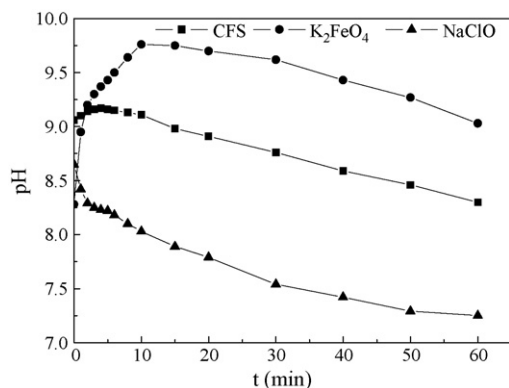
Fig. 8. pH change with reaction time in CFS, K_2FeO_4 and NaClO reaction systems. Conditions: CFS 25 mg L^{-1}; K_2FeO_4 25 mg L^{-1}; NaClO 20 mg L^{-1}; c_{X-3B} 0.08 mmol L^{-1}.

Fig. 9. TOC and COD removal percentage with time. Conditions: pH 8.5; COD 25.4 mg L^{-1}; TOC 8.84 mg L^{-1}; CFS 25 mg L^{-1}.

hand, some organic acids were generated during the degradation of X-3B. These acid substances would neutralize OH$^-$ ions and lower the pH value of the solution. The pH value decreased in CFS reaction system after 5 min and in K_2FeO_4 reaction system after 15 min. It indicated that the contribution of organic acids to the pH value was greater than that of OH$^-$ produced by Fe(VI). While for NaClO reaction system, there were only organic acids produced and the pH value decreased from the beginning of the reaction time.

3.7. Carbon mineralization

The reduction of TOC was monitored to evaluate the mineralization of the X-3B, as shown in Fig. 9. The initial TOC was 8.84 mg L^{-1}, COD was 25.4 mg L^{-1}. Fig. 9 showed that the removal percentage of TOC and COD were 4% and 24% after 10 min, and 9% and 42% after 60 min, respectively. However, the efficiency of decolorization was 95% (after 10 min) and 100% (after 60 min) (Fig. 3). It was indicated that color decay was considerably faster than the reduction of TOC and COD, which attributed to the ease of chromophore destruction. The data suggested that the mineralization percentage of X-3B by CFS was low and the mineralization was slow. It needs much longer contact for the conversion of TOC to CO_2.
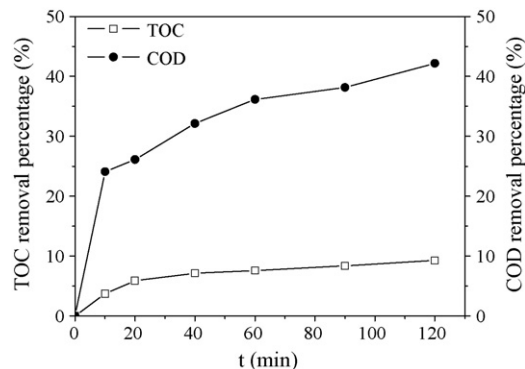
3.8. Intermediates analysis by GC/MS

The samples of X-3B oxidized for 1 min, 5 min, 15 min, 30 min and 60 min were combined to determine the intermediates by GC–MS after esterification, and the results were presented in Table 1. It could be presumed that naphthalene, 1-isocyanato-, azobenzene, phthalic acid, muconic acid, phenol and hydroquinone were main oxidation products. The organic acids as phthalic acid and muconic acid lowered the pH value of reaction solution, which was in accordance with Fig. 8.

On the basis of GC/MS analysis and previous work reported in the literatures [26,27], degradation pathway of X-3B oxidized by CFS was presumed and presented in Fig. 10. The first step was the breaking down of azo bond, C—N bonds between the azo group and benzene or naphthalene ring and C—N bonds between amido and naphthalene or triazine ring. Aniline-like and phenol-like compounds were formed during this step. Triazene was degraded with the Cl$^-$ production, and the naphthalene ring transformed to naphthalene, 1-isocyanato- and phthalic acid. At the same time, sulfonic groups began to be cut off from the naphthalene rings, accompanied with the formation of sulfate ions. Since aromatic ring structures and triazene are more difficult to be destructed, the elimination of these ring structures needs a longer time. For the azobenzene observed by the GC/MS, the azo dye-like molecules were released

Table 1
Main intermediates of X-3B identified by GC/MS

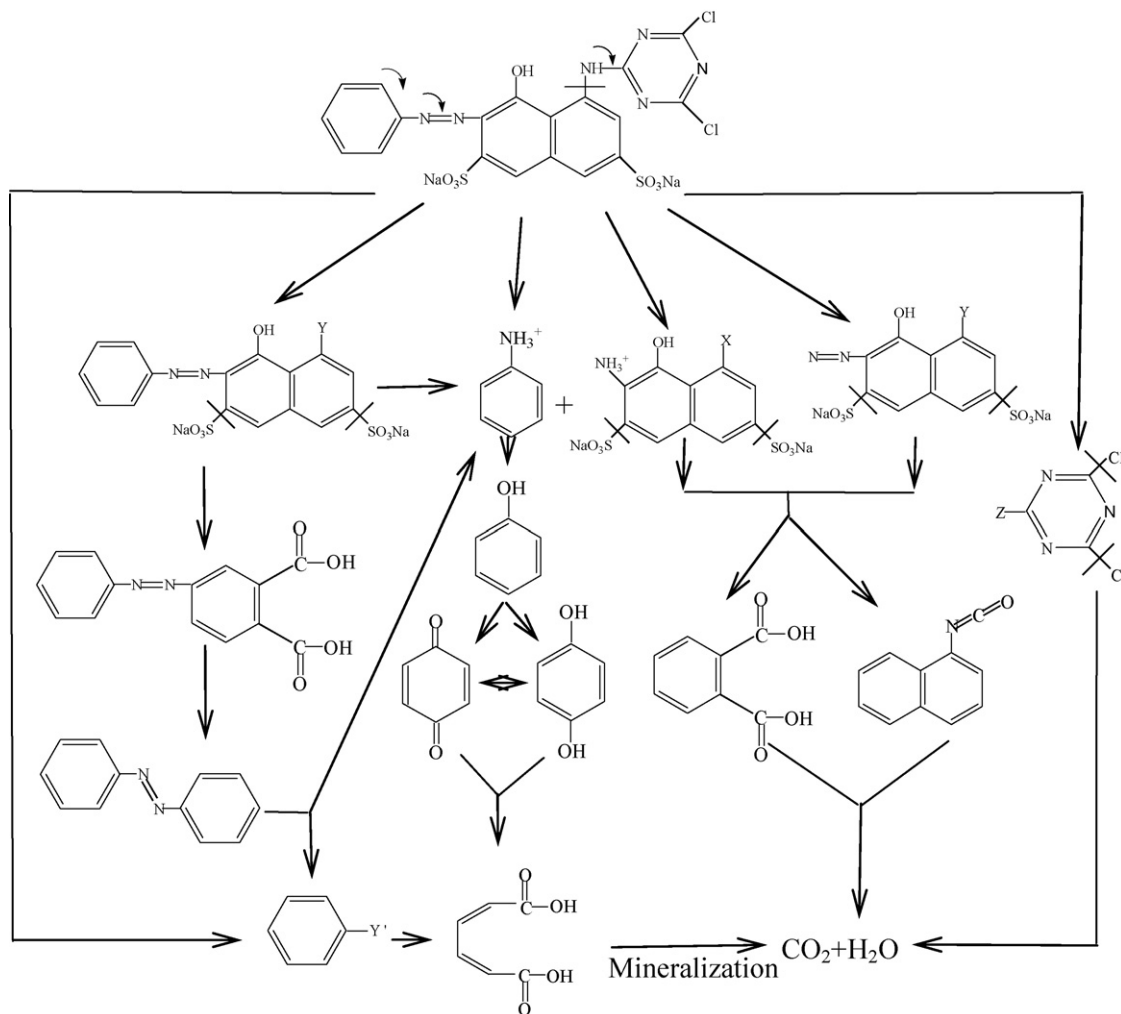| No.	Compounds	Formula	Structural formula
1	Phthalic acid, 4-methoxyphenyl phenyl ester	$C_{21}H_{16}O_5$	
2	Naphthalene, 1-isocyanato-	$C_{11}H_7NO$	
3	Dimethyl phthalate	$C_{10}H_{10}O_4$	
4	2,4-Hexadienedioic acid, dimethyl ester	$C_8H_{10}O_4$	
	Azobenzene	$C_{12}O_{10}N_2$	

Fig. 10. Degradation pathway of X-3B oxidized by CFS.

from the breaking of the C—N single bond between the amido and naphthalene. It was transformed to azobenzene, then the C—N bond or N=N bond cleaved to yield aniline or substituted benzene. The aniline and substituted benzene were further oxidized to yield muconic acid. The muconic acid would be further oxidized to produce carbon dioxide and water.

4. Conclusions

Composite ferrate solution with improved stability was successfully prepared in this study. The stability of Fe(VI) increased from 83% decomposition after 1 d for $0.29\,\text{mmol}\,L^{-1}$ pure ferrate potassium solution at pH 10 to 24% decomposition after 16 d for $1\,\text{mmol}\,L^{-1}$ Fe(VI) in CFS. The CFS is a strong oxidant and can degrade azo dye X-3B efficiently, because almost total decolorization was obtained. The degradation efficiency was strongly dependent on pH value, and the optimal pH range was pH 8.4–10.6. Initial dye concentration and CFS dosage also affected the degradation efficiency. The maximum oxidant load was 5.2–5.7 μmol X-3B/1 mg K_2FeO_4. The Fe(VI) and ClO^- contained in CFS had synergetic effect for the degradation of X-3B. The Fe(VI) appeared more effective in comparison with ClO^-. Organic acids such as phthalic acid identified by GC/MS lowered the pH value in the reaction solution. The TOC and COD removal percentage were 9% and 42%, respectively. It indicated that the complete mineral-

ization of X-3B could not be achieved under the oxidation by CFS. Based on the products identified and theoretical analysis, possible degradation pathway of X-3B was presumed. Under oxidative conditions, N=N cleavage and C—N cleavage were possible initial steps in the degradation of X-3B.

References

[1] X.L. Dong, W. Ding, X.F. Zhang, X.M. Liang, Mechanism and kinetics model of degradation of synthetic dyes by UV-vis/H₂O₂/ferrioxalate complexes, Dyes Pigments 74 (2) (2007) 470–476.
[2] Y.M. Dong, K. He, B. Zhao, Y. Yin, L. Yin, A. Zhang, Catalytic ozonation of azo dye active brilliant red X-3B in water with natural mineral brucite, Catal. Commun. 8 (2007) 1599–1603.
[3] Y. Liu, X. Chen, J. Li, C. Burda, Photocatalytic degradation of azo dyes by nitrogen-doped TiO₂ nanocatalysts, Chemosphere 61 (1) (2005) 11–18.
[4] M.A. Behnajady, N. Modirshahla, F. Ghanbary, A kinetic model for the decolorization of C.I. Acid Yellow 23 by Fenton process, J. Hazard. Mater. 48 (1–2) (2007) 98–102.
[5] A. Riga, K. Soutsas, K. Ntampegliotis, V. Karayannis, G. Papapolymerou, Effect of system parameters and of inorganic salts on the decolorization and degradation of Procion H-exl dyes. Comparison of H₂O₂/UV, Fenton, UV/Fenton, TiO₂/UV and TiO₂/UV/H₂O₂ processes, Desalination 211 (1–3) (2007) 72–86.
[6] M. Mahbubul Hassan, C.J. Hawkyard, Ferral-catalyzed ozonation of aqueous dyes in a bubble-column reactor, Catal. Commun. 3 (7) (2002) 281–286.
[7] D.E. Kritikos, N.P. Xekoukoulotakis, E. Psillakis, D. Mantzavinos, Photocatalytic degradation of reactive black 5 in aqueous solutions: effect of operating conditions and coupling with ultrasound irradiation, Water Res. 41 (10) (2007) 2236–2246.

[8] M. Faisal, M. Abu Tariq, M. Muneer, Photocatalysed degradation of two selected dyes in UV-irradiated aqueous suspensions of titania, Dyes Pigments 72 (2) (2007) 233–239.

[9] H. Zhang, L.J. Duan, D.B. Zhang, Decolorization of methyl orange by ozonation in combination with ultrasonic irradiation, J. Hazard. Mater. 138 (1–2) (2006) 53–59.

[10] R. Jain, S. Varshney, S. Sikarwar, Electrochemical techniques for the removal of Reactofix Golden Yellow 3 RFN from industrial wastes, J. Colloid Interface Sci. 313 (1) (2007) 248–253.

[11] J.Q. Jiang, S. Wang, A. Panagoulopoulos, The exploration of potassium ferrate(VI) as a disinfectant/coagulant in water and wastewater treatment, Chemosphere 63 (2) (2006) 212–219.

[12] J.Q. Jiang, Research progress in the use of ferrate(VI) for the environmental remediation, J. Hazard. Mater. 146 (3) (2007) 617–623.

[13] V.K. Sharma, R.A. Rendon, F.J. Millero, F.G. Vazquez, Oxidation of thioacetamide by ferrate(VI), Mar. Chem. 70 (1–3) (2000) 235–242.

[14] N. Graham, C.C. Jiang, X.Z. Li, J.Q. Jiang, J. Ma, The influence of pH on the degradation of phenol and chlorophenols by potassium ferrate, Chemosphere 56 (10) (2004) 949–956.

[15] Y. Lee, J. Yoon, U.V. Gunten, Kinetics of the oxidation of phenols and phenolic endocrine disruptors during water treatment with ferrate(Fe(VI)), Environ. Sci. Technol. 39 (22) (2005) 8978–8984.

[16] V.K. Sharma, Potassium ferrate(VI): an environmentally friendly oxidant, Adv. Environ. Res. 6 (2) (2002) 143–156.

[17] V.K. Sharma, D.B. O'Connor, Ferrate(V) oxidation of thiourea: a premix pulse radiolysis study, Inorg. Chim. Acta 311 (1–2) (2000) 40–44.

[18] M.D. Johnson, B.J. Hornstein, Kinetics and mechanism of the ferrate oxidation of hydrazine and monomethylhydrazine, Inorg. Chim. Acta 225 (1–2) (1994) 145–150.

[19] C. Li, X.Z. Li, N. Graham, A study of the preparation and reactivity of potassium ferrate, Chemosphere 61 (4) (2005) 537–543.

[20] Y. Lee, J. Yoon, U.V. Gunten, Spectrophotometric determination of ferrate (Fe(VI)) in water by ABTS, Water Res. 39 (10) (2005) 1946–1953.

[21] Y. Xu, Comparative studies of the $Fe^{3+/2+}$–UV, H_2O_2–UV, TiO_2–UV/vis systems for the decolorization of a textile dye X-3B in water, Chemosphere 43 (8) (2001) 1103–1107.

[22] T. Ernst, M. Wawrenczyk, M. Cyfert, M. Wronska, Effect of pH on the kinetics of ferrate(VI) decomposition, Bull. Acad. Pol. Sci. Ser. Sci. Chim. 27 (10) (1979) 773–778.

[23] T.M. Pizzolato, E. Carissimi, E.L. Machado, A.H. Schneider, Colour removal with NaClO of dye wastewater from an agate-processing plant in Rio Grande do Sul, Brazil, Int. J. Miner. Process 65 (3) (2002) 203–211.

[24] V.K. Sharma, Ferrate(V) oxidation of pollutants: a premix pulse radiolysis study, Radiat. Phys. Chem. 65 (4–5) (2002) 349–355.

[25] M.D. Johnson, K.D. Sharma, Kinetics and mechanism of the reduction of ferrate by one-electron reductants, Inorg. Chim. Acta 293 (2) (1999) 229–233.

[26] Y. Zhang, X.M. Dou, J. Liu, M. Yang, L.P. Zhang, Y. Kamagata, Decolorization of reactive brilliant red X-3B by heterogeneous photo-Fenton reaction using an Fe-Ce bimetal catalyst, Catal. Today 126 (3–4) (2007) 387–393.

[27] A. Gutowska, J. Kaluźna-Czaplińska, W.K. Jóźwiak, Degradation mechanism of Reactive Orange 113 dye by H_2O_2/Fe^{2+} and ozone in aqueous solution, Dyes Pigments 74 (1) (2007) 41–46.